Friction-stir welding of Al-Mg-Mn-Zr sheets by using a hemispherical tool

IOP Conf. Series: Materials Science and Engineering **672** (2019) 012040 doi:10.1088/1757-899X/672/1/012040

Friction-stir welding of Al-Mg-Mn-Zr sheets by using a hemispherical tool

I Vysotskiy, S Malopheyev, S Mironov and R Kaibyshev

Belgorod State University, Pobeda 85, Belgorod 308015, Russia

E-mail: malofeev@bsu.edu.ru

Abstract. A new design of the welding tool for friction-stir welding (FSW) was proposed. The main idea was in using of a hemispherical tool probe. Such a tool is very simple (and cost-effective) in fabrication and provides excellent mixing of the material during FSW, thus avoiding welding defects. In this work, the feasibility of this tool for joining of Al-Mg-Mn-Zr alloy and its effect on the microstructure and mechanical properties of the produced welds were studied.

1. Introduction

Friction-stir welding (FSW) is a relatively simple but very effective technology for solid-state joining of structural materials [1–6]. One of the key issues of FSW is the welding tool [1–6]. The tool provides material mixing during the welding process, and, thus governs the microstructure and service properties of the produced welds. To enhance the mixing process, tools of very complex design are sometimes used [3,5]. This facilitates the material flow, but increases the production cost. In the present work, however, an alternative approach in the tool designing was used. Based on the idea that the material flow during FSW is mainly disturbed by abrupt changes in the tool geometry, a spherical design of the tool was suggested to promote very smooth mixing of the material. On the other hand, tools of this design should be relatively simple (and thus cost-effective) in production. Therefore, a welding tool with a hemispherical tool probe was developed. In the previous works, the excellent welding performance of such a tool were shown during FSW of a TWIP-steel [7] and a high-entropy alloy [8]. The purpose of the present study was examination of feasibility of such a tool for joining of the Al-Mg-Mn-Zr alloy and its effect on the microstructure and mechanical properties of the produced welds.

2. Material and experimental procedure

The design of the developed tool is shown in figure 1a. Briefly, the tool consisted of a conventional concave-shaped shoulder of 12.5 mm in diameter, and a hemispherical-shaped probe of 2 mm in radius. The tool was fabricated from a W-Co-based alloy. This material is well recommended for joining of relatively high-strength materials, including steels [7-9] and titanium-based alloys.

The program material, i.e. a commercial AA5083 alloy with the chemical composition Al–5.4% Mg–0.5% Mn–0.1% Zr–0.12% Si–0.014% Fe (wt.%), was fabricated by direct chill casting and subsequent homogenization at 360 °C (633 K) for 6 h [10–12]. The homogenized material was subjected to equal-channel angular pressing (ECAP) at ~300 °C and a pressing rate of 3 mm/s to an accumulated true strain of ~12 by using the BCZ processing route. For this purpose, an isothermal die

with a rectangular cross-section and an intersection angle of 90° was used. To equilibrate the processing temperature during ECAP, the material was preheated for ~120 min prior to the first pass, whereas the preheating interval between subsequent passes was ~ 5 min. Following the final ECAP pass, the processed material was quenched in water. From the ECAPed material, sheets 10 mm thick were sliced and then rolled parallel to the ECAP direction at ambient temperature to a total thickness reduction of ~80 pct. This was achieved by multiple rolling passes, ~10 pct. of strain each. Following rolling, the produced sheets were annealed at 300 °C for 1 h. This rolled material was defined as the base material.

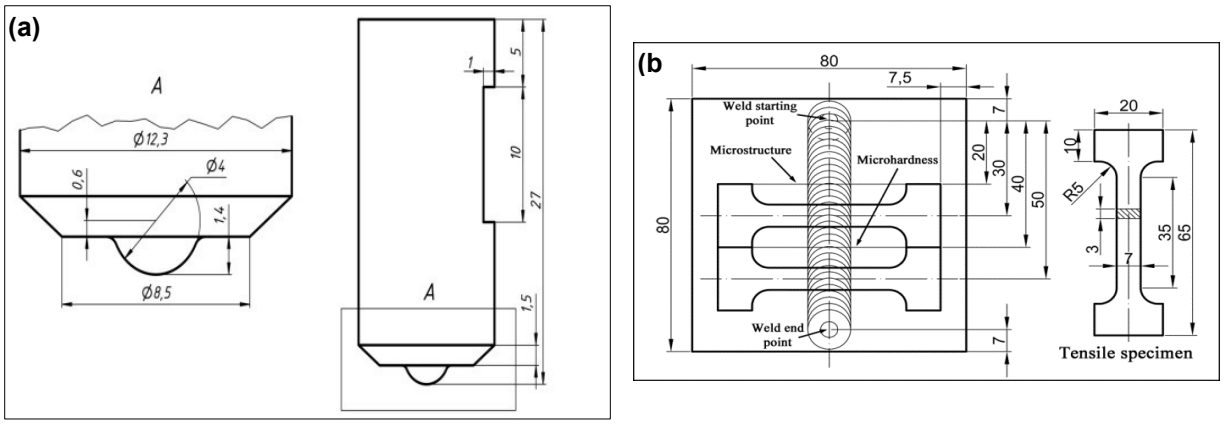

Figure 1. A schematic of the welding tool (a) and arrangement and dimensions of tensile specimens (b).

The obtained 2-mm-thick sheets were butt-welded parallel to the rolling direction using an AccuStir 1004 FSW machine. FSW was applied at a tool rotation of 500 rpm, a tool travel speed of 150 mm/min, and a tool tilting angle of 2.5°. The principal directions of the FSW geometry were denoted as the welding direction (WD), transversal direction (TD) and normal direction (ND). The obtained friction-stir welded material was defined as a joint.

Microstructural observations were performed mainly by electron backscatter diffraction (EBSD) technique and optical microscopy. The final surface finish was obtained by electro-polishing in a 25 pct. solution of nitric acid in methanol. EBSD analysis was conducted by using a FEI Quanta 600 field-emission-gun scanning electron microscope (FEG-SEM) equipped with TSL OIMTM software. In the EBSD maps shown, the low-angle boundaries (LABs) ($2°<\theta<15°$) and the high-angle boundaries (HABs) ($\geq 15°$) were depicted as red and black lines, respectively.

To examine the mechanical properties, axial tensile tests to failure were applied. The tensile specimens of the joint were centered at the weld centerline and included all characteristic microstructural zones of FSW. The dimensions of the specimens are shown in figure 1b. The tensile tests were conducted at ambient temperature and a constant cross-head velocity corresponding to a nominal strain rate of 10-3 s-1 by using an Instron 5882 universal testing machine. Other experimental details were reported elsewhere [10,12].

3. Results and discussion

3.1. Microstructure

A typical appearance of the microstructure of the base material in the ND×RD and ND×TD planes is shown in figure 2. The microstructure could be described in terms of a mixture of relatively-coarse pancake-shaped grains and fine equiaxed grains, thus being somewhat bimodal. Nevertheless, the mean grain intercept length was measured and found to be ~10 μm in the RD and ~6 μm along the ND.

Low-magnification optical observations of the transversal cross-section of the produced joint revealed no volumetric defects, thus confirming excellent performance of the developed welding tool. A typical microstructure evolved in the center of the stir zone is shown in figure 3. From a comparison with figure 2 it is clear that FSW led to significant microstructural changes. Specifically, the stir-zone microstructure was dominated by completely recrystallized fine grains with a mean size of ~1.4 μm and a fraction of HABs as high as 88% (figure 3).

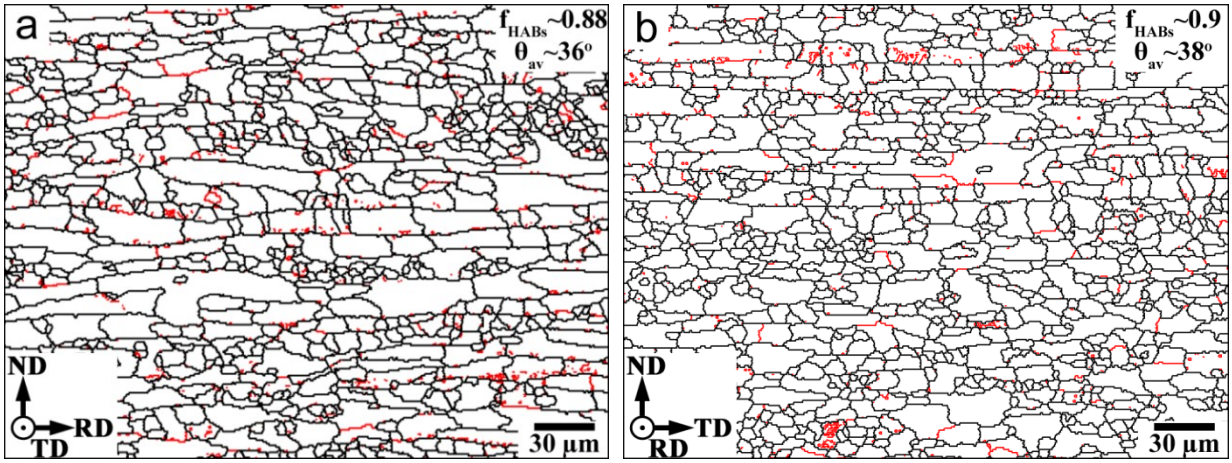

Figure 2. EBSD maps showing typical microstructure of *base material* in the ND×RD plane (a) and the ND×TD plane. The f_{HABs} and θ_{av} in the insets in the top right corner indicate the HABs fraction and the average misorientation, respectively.

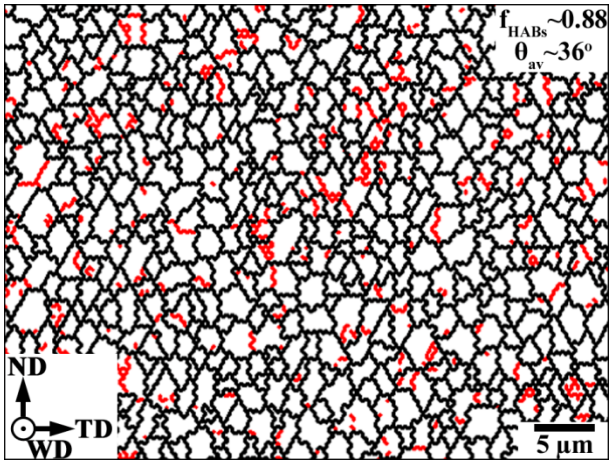

Figure 3. Typical microstructure in the center of the *stir zone*. The f_{HABs} and θ_{av} in the insets in the top right corner are the HABs fraction and the average misorientation, respectively.

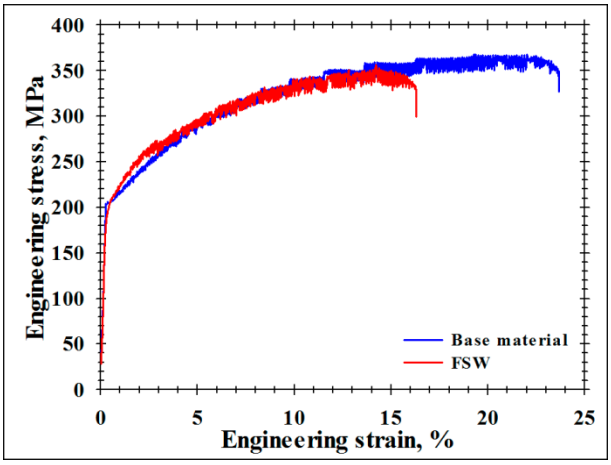

Figure 4. Typical deformation diagrams of the base material and the joint recorded during transverse tensile tests.

Table 1. Mechanical properties of the *base material* and the *joints*.

Material condition	Yield strength, MPa	Ultimate tensile strength, MPa	Ductility, %	Joint efficiency for UTS, %	Failure location
Base material	205	370	23	-	-
FSW	205	355	16	96	Heat-affected zone

3.2. Tensile properties

Typical deformation diagrams recorded during the transversal tensile tests of the base material and the joint are shown in figure 4. The relevant results of the tests are summarized in table 1. A characteristic feature of all deformation diagrams was the repeating oscillations indicating the serrated character of the material flow. This phenomenon is characteristic of Al-Mg alloys and is known as the Portevin-Le Chatelier (PLC) effect [10,13].

The produced joint demonstrated excellent mechanical properties. Specifically, the joint efficiency for the yield strength was 100% whereas that for the ultimate tensile strength was to 96% (figure 4, table 1). On the other hand, the joint exhibited relatively low ductility. This effect was associated with strain localization in the softest microstructural region of the weld, i.e. heat-affected zone, which led to premature failure of the weld.

4. Conclusions

In this work, the performance of a newly-developed welding tool with a hemispherical probe was examined. To this end, this tool was used for FSW of an Al-Mg-Mn-Zr alloy and its effect on the microstructure and mechanical properties was studied. The produced joint had no volumetric defects, and the efficiency of the joint in terms of strength characteristics was close to 100%. The microstructure generated in the stir zone was dominated by completely recrystallized fine grains with a mean size of ~1.4 μm and a high HAB fraction.

Acknowlegements

This study was financially supported by the Russian Science Foundation, grant No. 18-79-10174. The authors are grateful to the staff of the Joint Research Center, “Technology and Materials” Belgorod State National Research University for their assistance with the mechanical and structural characterizations.

References

[1] Threadgill P L, Leonard A J, Shercliff H R and Withers P J 2009 *Int. Mater. Rev.* **54** 49
[2] Aissani M, Gachi S, Boubenider F and Benkedda Y 2010 *Mater. Manuf. Process.* **25** 1199
[3] Palanivel R, Koshy Mathews P, Murugan N and Dinaharan I 2012 *Mater. Des.* **40** 7
[4] García-Bernal M A, Mishra R S, Verma R and Hernández-Silva D 2016 *Mater. Sci. Eng.* A **670** 9
[5] Elangovan K and Balasubramanian V 2008 *Mater. Des.* **29** 362
[6] Kumar K, Kailas S V, Srivatsan T S 2011 *Mater. Manuf. Process.* **26** 915
[7] Torganchuk V, Vysotskiy I, Malopheyev S, Mironov S and Kaibyshev R 2019 *Mater. Sci. Eng.* A **746** 248
[8] Shaysultanov D, Stepanov N, Malopheyev S, Vysotskiy I, Sanin V, Mironov S, Kaibyshev R, Salishchev G and Zherebtsov S 2018 *Mater. Charact.* **145** 353
[9] El-Batahgy AM, Miura T, Ueji R and Fujii H 2016 *Mater. Sci. Eng.* A **651** 904
[10] Malopheyev S, Kaibyshev R 2015 *Mater. Sci. Eng.* A **620** 246
[11] Nikulin I, Kipelova A, Malopheyev S and Kaibyshev R 2012 *Acta Mater.* **60** 487
[12] Malopheyev S, Vysotskiy I, Mironov S, Zhemchuzhnikova D and Kaibyshev R 2018 *AIP Conf. Proc.* **2051** 020186
[13] Lebyodkin M A, Zhemchuzhnikova D A, Lebedkina T A and Aifantis E C 2019 R*esults Phys.* **12** 867